

Road-departure prevention in an emergency obstacle avoidance situation

Katzourakis, D.; de Winter, J.C.F.; Alirezaei, M.; Corno, M.; Happee, R.

DOI

[10.1109/TSMC.2013.2263129](https://doi.org/10.1109/TSMC.2013.2263129)

Publication date

2014

Document Version

Final published version

Published in

IEEE Transactions on Systems, Man, and Cybernetics: Systems

Citation (APA)

Katzourakis, D., de Winter, J. C. F., Alirezaei, M., Corno, M., & Happee, R. (2014). Road-departure prevention in an emergency obstacle avoidance situation. *IEEE Transactions on Systems, Man, and Cybernetics: Systems*, 44(5), 621-629. <https://doi.org/10.1109/TSMC.2013.2263129>

Important note

To cite this publication, please use the final published version (if applicable).
Please check the document version above.

Copyright

Other than for strictly personal use, it is not permitted to download, forward or distribute the text or part of it, without the consent of the author(s) and/or copyright holder(s), unless the work is under an open content license such as Creative Commons.

Takedown policy

Please contact us and provide details if you believe this document breaches copyrights.
We will remove access to the work immediately and investigate your claim.

Green Open Access added to TU Delft Institutional Repository

'You share, we take care!' - Taverne project

<https://www.openaccess.nl/en/you-share-we-take-care>

Otherwise as indicated in the copyright section: the publisher is the copyright holder of this work and the author uses the Dutch legislation to make this work public.

Road-Departure Prevention in an Emergency Obstacle Avoidance Situation

Diomidis I. Katzourakis, Joost C. F. de Winter, Mohsen Alirezaei,
Matteo Corno, and Riender Happee

Abstract—This paper presents a driving simulator experiment, which evaluates a road-departure prevention (RDP) system in an emergency situation. Two levels of automation are evaluated: 1) haptic feedback (HF) where the RDP provides advisory steering torque such that the human and the machine carry out the maneuver cooperatively, and 2) drive by wire (DBW) where the RDP automatically corrects the front-wheels angle, overriding the steering-wheel input provided by the human. Thirty participants are instructed to avoid a pylon-confined area while keeping the vehicle on the road. The results show that HF has a significant impact on the measured steering wheel torque, but no significant effect on steering-wheel angle or vehicle path. DBW prevents road departure and tends to reduce self-reported workload, but leads to inadvertent human-initiated steering resulting in pylon collisions. It is concluded that a low level of automation, in the form of HF, does not prevent road departures in an emergency situation. A high level of automation, on the other hand, is effective in preventing road departures. However, more research may have to be done on the human response while driving with systems that alter the relationship between steering-wheel angle and front-wheels angle.

Index Terms—Drive by wire (DBW), driving simulation, emergency maneuver, haptic feedback (HF), road-departure prevention (RDP), shared control, steering assist, steering force feedback.

Manuscript received March 29, 2012; revised December 11, 2012; accepted April 6, 2013. Date of publication July 31, 2013; date of current version April 11, 2014. The work of D. Katzourakis was supported by the SKF Automotive Development Center, Nieuwegein, The Netherlands. The work of J. C. F. de Winter was supported by the Dutch Technology Foundation, Applied Science Division of the Netherlands Organization for Scientific Research, and the Technology Program of the Ministry of Economic Affairs. This paper was recommended by Editor A. Bargiela.

D. Katzourakis is with the CAE Active Safety and Vehicle Dynamics Group, Research and Development, Volvo Cars Corporation, Göteborg 40531, Sweden (e-mail: diomidis.katzourakis@volvocars.com).

J. C. F. de Winter is with the Department of BioMechanical Engineering, Faculty of Mechanical, Maritime and Materials Engineering, Delft University of Technology, 2628 CD Delft, The Netherlands (e-mail: j.c.f.dewinter@tudelft.nl).

M. Alirezaei is with the Delft Center for Systems and Control, Faculty of Mechanical, Maritime and Materials Engineering, Delft University of Technology, 2628 CD Delft, The Netherlands (e-mail: m.alirezaei@tudelft.nl).

M. Corno is with the Delft Center for Systems and Control, Faculty of Mechanical, Maritime and Materials Engineering, Delft University of Technology, 2628 CD Delft, The Netherlands, and also with IAS Group, Dipartimento di Elettronica e Informazione, Politecnico di Milano, Milan 20133, Italy (e-mail: m.corno@tudelft.nl).

R. Happee is with the Biomechanical Engineering Research Group, Faculty of Mechanical, Maritime, and Materials Engineering, TU Delft, 2628 CD Delft, The Netherlands (e-mail: r.happee@tudelft.nl).

Color versions of one or more of the figures in this paper are available online at <http://ieeexplore.ieee.org>.

Digital Object Identifier 10.1109/TSMC.2013.2263129

I. INTRODUCTION

LANE departure is a factor in a large proportion of accidents involving fatal or serious injuries, and is usually induced by the driver's inattention, fatigue, impairment and distraction, or improper control inputs in an emergency situation. Jermakian [1] estimated the potential of lane-departure warning (LDW) systems and asserted that lane departure appears relevant in 179 000 crashes per year, and related up to 7500 fatal crashes per year in the United States.

Since 2001, Nissan Motors in Japan has been offering a lane-keeping support system [2] enabled when the vehicle begins crossing the lane markings (Nissan Cima, [3]). In 2002 and 2003, Toyota [4] and Honda [5] launched their lane-keeping assist systems that apply steering-wheel torque to help drivers to keep the vehicle in the lane. Nowadays, many high-end automobile manufacturers (e.g., Mercedes, Volvo, BMW, Nissan-Infiniti, and Honda) offer similar assist systems in their top-class models. Most LDW systems utilize a camera to track road markings and estimate the vehicle's position relative to the road. The feedback to the driver varies from audible, visual, and/or vibrotactile signals, to haptic steering-wheel feedback. Nissan (Infiniti) was the first to offer lane-departure prevention (LDP), an extension of LDW [6]. In addition to the warning system, which is automatically enabled when the vehicle is started, LDP brakes slightly to help prevent unintended departure from the traveling lane. Due to the active intervention of LDP, Infiniti decided to require drivers to enable the system themselves. Infiniti predicts that if LDP were fitted to all vehicles, some 12% of all road fatalities could be annually prevented [7].

A study on a lateral drift warning system by the U.S. Department of Transportation [8] showed that drivers improved their lane keeping, spent 63% less time outside the lane, and increased their use of turn signals. Drivers readily accepted this system, viewing it as an easy and comfortable way to increase safety. Interestingly, drivers rated this system as useful but less satisfying compared to adaptive cruise control (ACC). Braitman *et al.* [6], using telephone interviews to owners of Infiniti vehicles equipped with LDW and LDP, investigated drivers' use and acceptance of these systems. The majority of the interviewees reported that they disliked nothing about the LDW system and stated that they drifted from the lane less often. As for the LDP system, 50% reported that they disliked nothing about it; 68% reported that they drifted less

and 22% were unaware that they were using LDP technology. The aforementioned statistics indicate that the LDW and LDP systems are appreciated by drivers.

LDP systems have gained attention in academic research. Studies on vibrotactile feedback for collision mitigation [9] and lane keeping [10] have yielded promising results. Griffiths and Gillespie [11] have explored the benefits of augmented force-feedback to share control between the driver and automated steering to support lane keeping. Mulder *et al.* [12] proposed a haptic guidance system, where the driver and support system share steering control, showing that continuous haptic support is an efficient way to support drivers during curve negotiation. This assertion concurs with the continuous haptic steering-support system for obstacle avoidance designed by Penna *et al.* [13]. Their proposed system reduced the number of crashes, control effort, and activity in critical situations. A literature review by De Winter and Dodou [14] argued that the effects of haptic-shared control [15] during routine tasks are now adequately established, but that more research needs to be done regarding safety-critical maneuvers.

Several studies tend to favor human-centered automation, where the driver always has control and authority of the vehicle, solely receiving feedback guidance on the steering wheel [12], [13]. However, the literature is still debating the required level of automation for a given driving task. A high level of automation may be preferable because of human limitations in speed and decision making [16]–[18]. An example of driver-assist technology deviating from the principle of human-centered automation (in the sense that it can act automatically in emergencies and override the driver, i.e., a high level of automation) is a collision-mitigation system that can apply the brakes if the driver does not act in time. If such a high level of automation was not entirely effective, it would not prevent collisions in all circumstances, and could increase collision risk when operated by a driver with miscomprehension of its functionality [17]. Research related to ACC [19], [20] agrees that automation has its pitfalls; although ACC is acknowledged to reduce mental workload, it has also been blamed for provoking false reliance on the system [20]. According to Seppelt *et al.* [19], reliance on ACC disengaged drivers from their primary task (driving) and increased their response time to vehicles braking ahead.

Summarizing, a high level of automation can lead to false reliance and/or miscomprehension of the functionality, which could reduce its potential benefits under certain conditions [17]. This suggests that careful design and empirical testing is essential for emergency situations (additional to normal driving); see, for instance, the study by Itoh *et al.* [21] presenting a pedestrian collision-avoidance system in emergency situations.

Although numerous studies have shown the potential of lane keeping and LDP systems [7]–[9], [12], [13], including drive-by-wire (DBW) approaches [22], there are few studies related to their effects during driver-in-the-loop emergency maneuvers.

The aim of this research is to investigate different levels of automation in an emergency scenario in conjunction with a road-departure prevention (RDP) system. The systems were

tested with 30 participants in a driving simulator. The RDP system utilizes look-ahead information to derive the future lateral position of the vehicle with respect to the road. The RDP system intervenes by applying haptic (advisory) feedback torque or correcting the angle of the front wheels (DBW) when road departure is likely to occur. A RDP controller developed by Alirezaei *et al.* [23] determines the correcting steering input using the driver's steering input and the vehicle's driving speed (similar to [11], [12], and [24]).

Four steering setups were evaluated in an emergency obstacle avoidance scenario; a setup without support was tested first, followed by three support setups tested in randomized order.

- 1) *No support*: normal driving.
- 2) *Haptic feedback (HF)*: if a road departure is likely to occur, the RDP applies an advisory steering torque such that human and machine carry out the emergency maneuver cooperatively.
- 3) *DBW*: if a road departure is likely to occur, the RDP adjusts the front-wheels angle to keep the vehicle on the road, effectively overriding the driver.
- 4) *Combined (DBW & HF)*: if a road departure is likely to occur, the RDP both adjusts the front-wheels angle and applies a steering torque.

This study is the first to address the DBW concept for RDP in an emergency situation, building on initial results presented in [25]. Section II addresses the methods, the test apparatus, the RDP controller's operating principle, the steering support setups, the driving task and test group, and the statistical analysis. The results are analyzed in Section III and a discussion in Section IV concludes the paper.

II. METHODS

A. Test Apparatus

Driver-in-the-loop testing of the RDP controller was performed in fixed-base configuration of the X-Car driving simulator [26]. The simulator is based on a dSPACE real-time computer and runs a vehicle-dynamics model from the dSPACE automotive simulation model package. The vehicle is an open MATLAB/Simulink model with 24 degrees of freedom. It incorporates semi-empirical tire models, suspension dynamics, and steering system model. Steering force feedback is delivered through a brushless three-phase motor, evaluated for its high fidelity in conjunction with its controllers [26]. Three TFT monitors composed a viewing angle of 135°.

The simulated vehicle, with front-wheel drive, mild understeer, 1200 kg of mass, and 2500 kg m² of yaw inertia, is assumed to utilize a camera for measuring the road boundary which is used to predict the vehicle lateral offset y_{la} (see Fig. 1).

B. RDP Controller

The RDP system [23] is shown as a block diagram in Fig. 2. Assume that $\delta_c = 0$ and that y_{la} is within the road limits; then, $y_d = y_{la}$, and therefore, $y_{in} = 0$. In this case, the controller has no effect on the vehicle and $\delta_c = 0$. If the driver's steering input

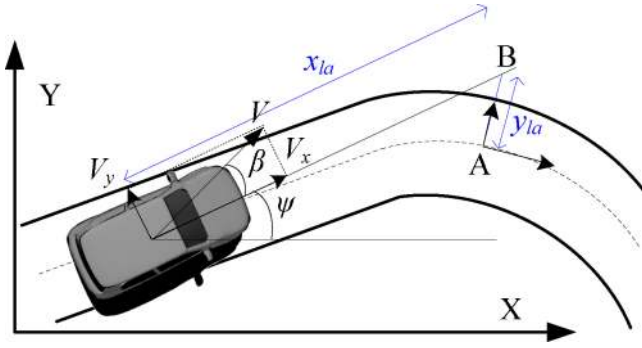


Fig. 1. RDP concept. Whether the car turns or the on-coming road becomes curvy, the road prevention scheme is the same. The normal to the road line from point A intersects at point B with the line parallel to the vehicle's longitudinal velocity vector V_x , x_{la} meters ahead. The distance y_{la} between points A and B represents the predicted lateral offset.

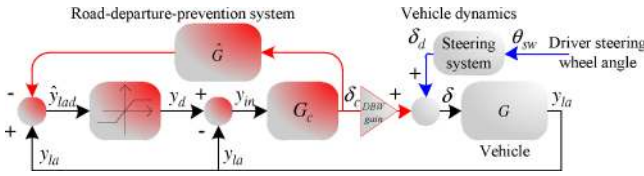


Fig. 2. RDP control scheme. Block G represents the vehicle dynamics from the front-wheels steering angle δ to y_{la} ; \hat{G} is a simplified vehicle dynamics model used to predict effects of current steering actions on the future lateral position. The predicted lateral position y_{la} is computed as in (1) where δ_c is the G_c controller's correcting angle and δ_d is the front-wheels steering angle deriving from the driver's steering-wheel angle θ_{sw} . The estimated desired lateral offset \hat{y}_{lad} is given in (2). The desired lateral offset y_d , saturated by the road limits, is given by (3) where y_L denotes the lateral limit (related to the road width). The input y_{in} to the G_c controller is given by (4).

δ_d points the vehicle outside the lateral limit y_L , the result is that $y_d \neq y_{la}$, inducing the controller G_c to become active ($\delta_c \neq 0$). The Simulink model from dSPACE (G), described at the start of Section II, calculates the future position of the vehicle and corresponding lateral offset with respect to the road. The RDP system in Fig. 2 is fed with the y_{la} signal deriving from the vehicle-dynamics model. The look-ahead time was set to 0.7 s, determining the preview length $x_{la} = 9.72$ m at 50 km/h (see Fig. 1). This time was appointed with pilot tests to offer driving comfort and RDP efficiency. For more details on the design of the G_c controller, we refer to the work by Alirezaei *et al.* [23]

$$y_{la} = G \cdot \delta \xrightarrow{\text{when DBW gain}=1} \longrightarrow y_{la} = G \cdot (\delta_c + \delta_d) \quad (1)$$

$$\hat{y}_{lad} = y_{la} - \hat{G} \cdot \delta_c \quad (2)$$

$$y_d = \begin{cases} -y_L, & \text{if } (\hat{y}_{lad} < -y_L) \\ \hat{y}_{lad}, & \text{if } (|\hat{y}_{lad}| \leq y_L) \\ y_L, & \text{if } (\hat{y}_{lad} > y_L) \end{cases} \quad (3)$$

$$y_{in} = y_d - y_{la} \quad (4)$$

C. Four Test Setups

Four steering setups were used to evaluate the RDP during an emergency maneuver and to explore the

differences between advisory (HF) and authoritarian support (DBW, DBW & HF):

- 1) *No support*: the RDP system is inactive and a mechanical connection is assumed between the steering wheel and the front wheels. The steering force feedback offered in this setup is derived from nonlinear tire simulation.
- 2) *HF*: the RDP system is active; a fixed mechanical connection is assumed between the steering wheel and front wheels. This setup applies an advisory HF torque, assisting the driver to avoid road departure. The driver may disregard the feedback by resisting the applied force. Haptic torque is the product of the correcting angle δ_c provided by the RDP, the steering ratio (steering_ratio $\approx \theta_{sw}/\delta$), and a haptic stiffness term. In an emergency maneuver, the correcting angle δ_c can increase quickly, inducing high-magnitude HF torques. Therefore, the haptic stiffness was limited to 0.5 Nm/rad. The force feedback offered in this setup is identical to the no-support condition during normal driving (when $\delta_c = 0$).
- 3) *DBW*: the RDP system is active; this setup allows decoupling of the steering wheel from the wheels, thus giving an extra degree of freedom to assist the driver. It imposes a corrective steering angle δ_c on the driver's input δ_d (see Fig. 2) resulting in a front-wheels steering angle δ (DBW gain = 1) that prevents road departure (even if the driver commands a deliberate road departure). When the driver steers back in the direction that will keep the vehicle within the road limits, then δ_c again becomes 0 and the steering angle δ is again equal to the driver's input. Effectively, this means that the RDP system compensates for all driver-steering actions leading to road departure, without the driver obtaining any HF on the RDP's activity. The steering force feedback offered in this setup is a product of a speed-related stiffness term K_s , the longitudinal velocity V_x , and the steering-wheel angle θ_{sw} (a relatively often-used approach to calculate steering force feedback in driving simulators). K_s was selected to offer similar force-feedback magnitude levels as the no-support setup.
- 4) *Combined (DBW & HF)*: this setup operates identically to the DBW setup in terms of compensating driver's steering input that will induce road departure, and offers an advisory HF torque guiding the driver to steering angles that will prevent road departure. A driver may override the feedback and can still adjust the steering-wheel angle θ_{sw} (see Fig. 2). The G_c controller though will impose a corrective angle δ_c if θ_{sw} points the vehicle outside the lateral limit. The steering force feedback during normal driving ($\delta_c = 0$) is derived from nonlinear tire simulation. The HF abbreviation in this setup denotes that there is HF information to the driver about the system's activity in the direction that the RDP controller is steering; it is therefore different from the HF setup explained above.

The four steering setups are described analytically in [25].

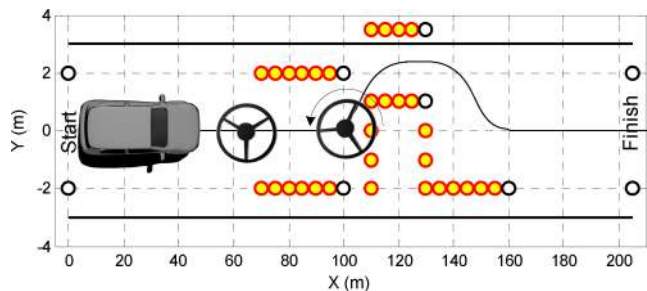


Fig. 3. Driving task. The vehicle started with 0 km/h and automatically accelerated up to a fixed speed of 50 km/h (reached around $x \approx 30$ m). The drivers were instructed to drive straight down the middle of the road (width=6 m; $y = [-3:3]$ m) and to steer at the end of the pylon-confined passage ($x = 100$ m). They had to pass through a 2.5-m-wide pylon passage from $x = [110:130]$ m, avoid departing the road and hitting the pylons, then return to the middle of the road and drive up to the finish line, 205 m away from the start. If the RDP was enabled, it supported drivers to stay on the road, but did not help to avoid the pylons.

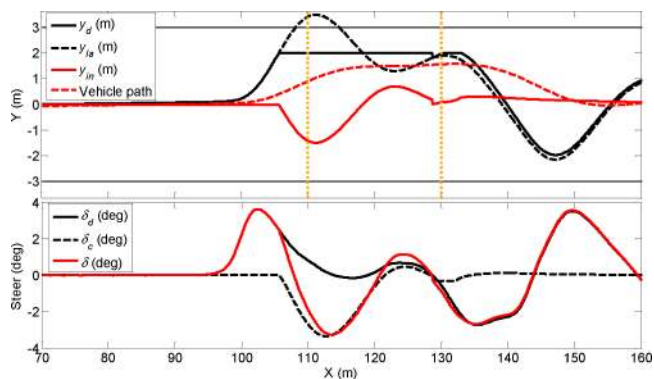


Fig. 4. Example of a DBW setup run. The top subplot shows the vehicle's path, the input y_{in} to the G_c controller as well as the future lateral y_{la} and future desired lateral y_d offset correspondingly. The bottom subplot displays the front-wheels angle δ , the RDP controller's correcting angle δ_c , and the driver's front-wheels steering angle δ_d derived from the steering-wheel angle θ_{sw} (see Fig. 2). Vertical lines ($x = 110$ m and $x = 130$ m) mark the area containing the obstacle.

D. Test Procedure and Driving Task

To induce the risk of road departure during an evasive maneuver, the test participants were asked to avoid a pylon-confined area (obstacle) and keep the vehicle within the road limits $y = [-3:3]$ m. The driving task is portrayed in Fig. 3.

E. RDP Principle of Operation: Example

Fig. 4 illustrates the principles of operation of the DBW setups (DBW and DBW & HF). The plot derives from the driving task presented in Section II-D. Initially, the G_c controller is inactive and the front-wheels steering angle δ equals to δ_d (deriving from the steering-wheel angle θ_{sw} ; Fig. 2). After $x = 97$, the driver turns the steering wheel to the left to avoid the obstacle between $x = 110$ m and $x = 130$ m (the area is marked with vertical lines). This action induces the future lateral offset y_{la} to exceed the future desired lateral offset y_d (having an upper limit y_L of 2 m) at $x \approx 105$ m. From this point on, $y_{in} \neq 0$ (4), which induces the controller G_c to generate the correcting angle δ_c to prevent the predicted road departure. The resulting front-wheels angle δ will keep the

vehicle within the road limits. After $x \approx 120$, the controller's correcting angle δ_c fades away since no further intervention is required, and δ becomes equal to δ_d .

F. Participants and Experiment Setup

From the 30 test participants, two were female and all but one had a driver's license. The mean age was 29.7 years ($SD = 5.0$), their average self-reported driven number of kilometers per year was 10095 ($SD = 10980$), and the average self-reported driving license possession was 9.0 years ($SD = 6.2$). All drivers graded their own driving competence, resulting in a mean score of 6.93 ($SD = 1.08$) on a scale from 1 (incompetent driver) to 10 (expert driver).

All drivers drove all four setups, with no support always driven first and the other three setups driven in random order. The operating principle of each setup was explained before testing began. The first 20 drivers practiced no support for 10 runs and the other setups for eight runs. Their performance was recorded on three additional runs. The remaining 10 drivers practiced no support for eight runs and the other setups for six runs. Their performance was recorded on seven additional runs as during the experiment we decided that analyzing more runs would enhance data reliability.

After completing a session with a steering support system, the participant stepped out of the simulator to fill in the NASA task load index (TLX). This questionnaire measures workload on six dimensions (mental demand, physical demand, temporal demand, performance, effort, and frustration) [27], and has been used in shared control car driving experiments before [28].

G. Statistical Analysis

The percentiles (medians, and 5th and 95th percentiles) and averages were used for statistical analysis of the collected data. Percentiles were calculated on all runs of all 30 drivers aggregated and averages were calculated first per participant and then across all 30 participants. Statistical significance of the results was assessed with paired t -tests, performed at the 1% significance level. The data were rank transformed [29] prior to submitting to the t -test, for higher robustness and to increase statistical power in the presence of possible outliers.

III. RESULTS

A. Objective Evaluation

Fig. 5 shows the vehicle's lateral position relative to the lane center for all four setups (medians, 5th and 95th percentiles). During initiation of the evasive maneuvers, the trajectories coincide. Around $x > 110$ m, the RDP predicts an on-coming road departure and intervenes according to the considered setup. HF (see HF versus no support) had no noteworthy effect, whereas DBW had a large effect (see DBW versus no support, and DBW & HF versus HF). Participants using DBW drove more to the right between $x = 110$ and 130 m, appeared to have steered left around $x \approx 125$ m, and were slower to return to lane center (see $x > 140$ m).

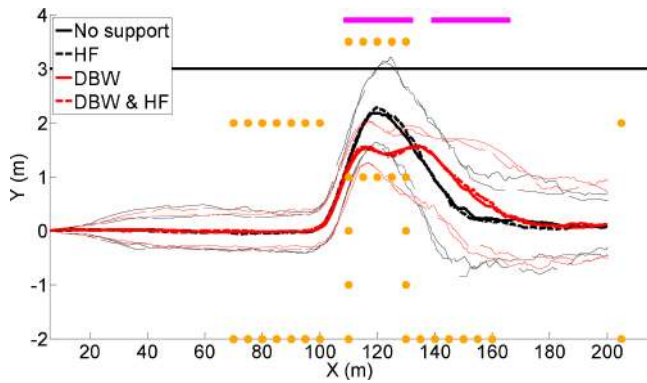


Fig. 5. Vehicle path: medians (thick lines), and 5th and 95th (thin lines) percentiles for the four setups (positive=to the left). The horizontal line at $y = 3$ m represents the road boundary. Bars are visible on top when HF versus DBW & HF (magenta) and DBW versus DBW & HF (red) are statistically significant (only magenta bars are visible here).

TABLE I

RUN PERCENTAGES WITH ROAD DEPARTURES AND PYLON HITS (FIRST CALCULATED PER PARTICIPANT AND THEN AVERAGED OVER ALL 30 PARTICIPANTS)

	Road-departure runs (%)	Pylon hit runs (%)
No support	52.9	29.5
HF	57.5	20.3
DBW	0.95	43.3
HF & DBW	0.48	44.4

The run percentages with road departures and pylon hits are given in Table I. The DBW setups (DBW and DBW & HF) highly reduced the number of road departures but increased the occurrence of crashes with the pylons representing the obstacle. Only four drivers experienced no departures in any condition. A run was considered a road departure when the y -coordinate of vehicle center of gravity (CG) exceeded 2.22 m ($y > 2.22$ m; the track width of the vehicle was 1.56 m and the road boundary was 3 m). A run was considered a pylon hit when the CG cross-sectioned a pylon array.

Fig. 6 shows medians, and 5th and 95th percentiles of the steering-wheel angle θ_{sw} for the four setups. These results confirm that HF had no noteworthy influence, whereas the DBW and DBW & HF setups had a large and significant effect. When a mechanical connection is assumed in the steering system (i.e., the no support and HF setups), the participants adopted a classical double pulse to avoid the obstacle. With the DBW and DBW & HF setups, drivers steered less to the right, between $110 < x < 120$, while making a second steering pulse to the left (around $x \approx 125$ m), presumably to avoid hitting the pylons positioned at $y = 1$ m. This was related to the fact that the RDP system would steer the front wheels to prevent road departure earlier than the drivers, minimizing the need for right steering (starting around $x \approx 100$ m). Possibly, certain drivers did not perceive the operating principle of the RDP (which was explained to them prior to testing) and their high magnitude second steering pulse overshoot the system, driving the cars toward the pylons (at $y = 1$ m) necessitating the observed third corrective left-steering input around $x \approx 125$ m.

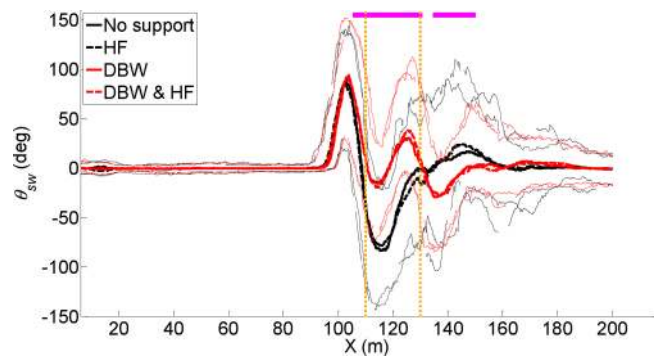


Fig. 6. Steering-wheel angle θ_{sw} : medians (thick lines), and 5th and 95th (thin lines) percentiles for the four setups (positive=to the left). The vertical lines ($x = 110$ m and $x = 130$ m) mark the first and last pylon that had to be avoided. Bars are visible on top when HF versus DBW & HF (magenta) and DBW versus DBW & HF (red) are statistically significant (only magenta bars are visible here).

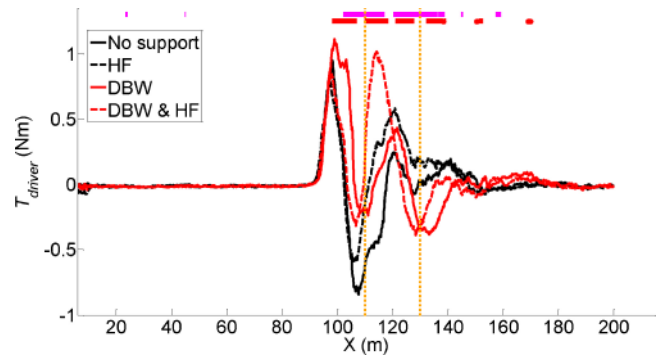


Fig. 7. Drivers' torque T_{driver} : medians for the four setups (positive to the left). Vertical lines ($x = 110$ m and $x = 130$ m) mark the first and last pylon that had to be avoided. Bars are visible on top when HF versus DBW & HF (magenta) and DBW versus DBW & HF (red) are statistically significant (the magenta bars are shown above the red).

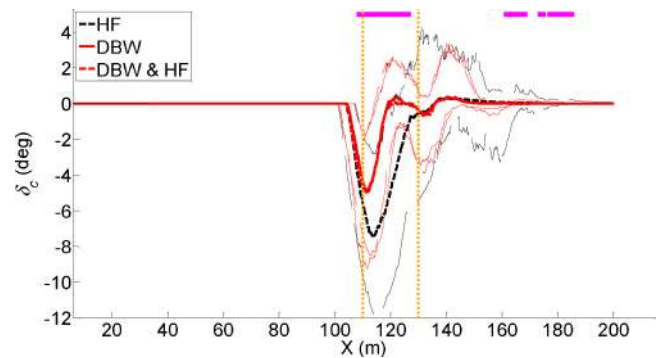


Fig. 8. Correcting angle δ_c : medians (thick lines), and 5th and 95th (thin lines) percentiles. Vertical lines ($x = 110$ m and $x = 130$ m) mark the first and last pylon that had to be avoided. Bars are visible on top when HF versus DBW & HF (magenta) and DBW versus DBW & HF (red) are statistically significant (only magenta bars are visible here).

Fig. 7 shows the medians of drivers' torque T_{driver} for all four setups. HF influenced the measured torques significantly. The second steering pulse can be seen again for DBW (around 125 m for DBW; and around 115 m for DBW combined with HF).

Fig. 8 displays the medians, and 5th and 95th percentiles of the correcting angle δ_c for the supporting setups. The

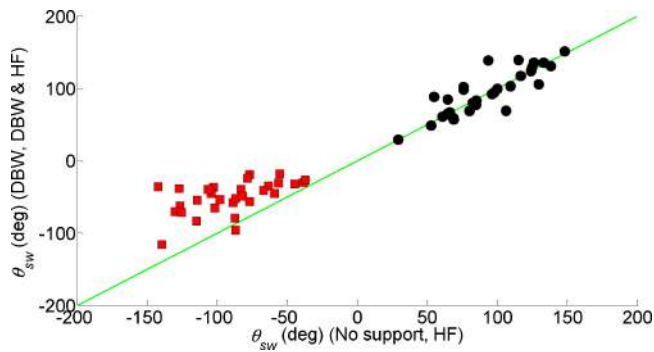


Fig. 9. Individual differences in maximum (black circles: left steering) and minimum (red squares: right steering) steering wheel angle. The values were calculated by averaging the runs of no support and HF, and by averaging the runs of DBW and DBW & HF.

magnitude of the δ_c angle for the HF setup, as well as its variability from the median, is considerably higher compared to the DBW setups. The median path of the HF setup (see Fig. 5) was closer or beyond the road limits, compared to the DBW setups, which in turn results in a greater input signal y_{in} [see (4)] to the G_c controller; this is translated to a greater correcting angle.

Fig. 9 shows individual differences in steering behavior. The initial steering pulse to the left (i.e., positive steering angles) shows marked individual differences, with some drivers having a smooth steering input and others having a relatively aggressive steering input, with average maximum steering angles as high as 150° . The Pearson [30] correlation of the maximum steering angle between no support and HF versus DBW and DBW & HF is high ($r=0.86$, $p < 0.001$, $n=30$), indicating that steering behavior is governed by reliable individual differences.

The steering to the right (negative steering angles) is clearly less for the DBW setup than for the no support and HF setup (see Fig. 9). This can be explained by the fact that the DBW systems automatically turn the front wheels to the right such that the drivers do not have to steer much to the right themselves.

The Pearson correlation between the maximum steering wheel angle and the minimum steering wheel angle was -0.90 ($p < 0.001$, $n=30$) for the no support and HF setup combined. This indicates that lane changes not supported by DBW show a relatively symmetric double-pulse pattern. For the DBW and DBW & HF conditions combined, the corresponding correlation was substantially weaker ($r=-0.52$, $p=0.003$, $n=30$). This indicates that the amount of steering required by drivers did not closely correspond to their initial steering input, and may be related to the extra steering pulse for the DBW conditions (see Fig. 6).

To evaluate the impact of each setup on the driving task, we employed a penalty-based analysis. An individual run accumulated penalty according to how much it deviated from the given task. The penalty map in Fig. 10 (bottom) shows the penalty values (represented in shades of gray) as a function of the x - and y -coordinates. The darker the shade, the greater the absolute penalty value (increasing linearly per shade area;

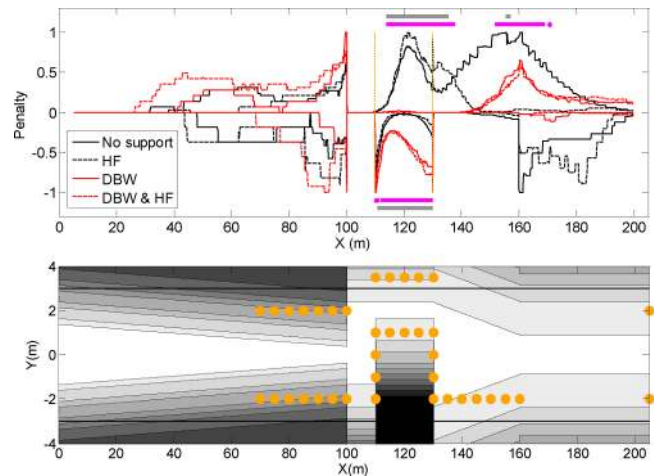


Fig. 10. Average penalty for the four setups for all driven maneuvers (top). Penalty map as a function of x - and y -coordinates; yellow dots represent the pylons (bottom). The darker the shade, the greater the absolute penalty value (increasing linearly per filled area; white area denotes zero penalty; the map accounts for the 1.56-m track width of the vehicle; thus, the penalty areas due to the pylons or the road limits extend inward toward the white area). Positive values are used above, and negative values below the white area on the map. The top subplot presents pointwise averages of positive points (vice versa for the negative). Averages were normalized (in the 0–1 scale) per task section: 0–100 m, 100–110 m, 110–130 m, 130–160 m, and 160–205 m. The positive–negative scheme distinguishes the task deviation with respect to the white area in the map; for example, in section 110–130 m, it shows that for DBW and DBW & HF, drivers accumulated penalty from the pylon side (negative points), while in the no support and HF setups, drivers accumulated penalty primarily by road departure (positive points). Bars are visible when HF versus DBW & HF (magenta) and no support versus DBW (gray) are statistically significant (the magenta bars are shown closer to the middle of the plot).

white area denotes zero penalty). To distinguish between deviation events (road departure versus pylon hit), the area to the (driver's) left of the ideal trajectory gets positive penalty values, while the area to the (driver's) right gets negative values; more specifically, positive values are used above, and negative values below the white area on the map. The driving task was divided into five task sections: 0–100 m, 100–110 m, 110–130 m, 130–160 m, and 160–205 m.

The top subplot of Fig. 10 shows the average penalty for the four setups for all driven maneuvers determined through the penalty map (bottom). These averages were normalized in the 0–1 scale by dividing with the maximum in magnitude penalty value per task section. The important part of this figure lies in the task section $x=110$ –130 m. The no support and HF setups mainly accumulated penalty through road departure (positive points), while the DBW and DBW & HF setups accumulated penalty primarily by hitting the pylons on the right (negative points). Both 110–130 m and 130–160 m task sections contain statistically significant results; HF versus DBW & HF (magenta) and no support versus DBW (gray). The remark made earlier for Fig. 5 that with DBW participants were slower to get back to lane center for $x > 140$ m (thus accumulating penalty) can also be seen in Fig. 10. The no support and HF setups have high penalty values for $x > 140$ m (compared to the DBW setups) due to few runs deviating drastically from the instructed task.

TABLE II
MEANS (STANDARD DEVIATIONS BETWEEN PARENTHESES) OF THE NASA TLX

	Mental demand	Physical demand	Temporal demand	Performance	Effort	Frustration
No support	12.0 (3.8)	8.5 (3.9)	11.9 (5.2)	10.9 (3.2)	12.7 (3.2)	8.4 (5.1)
HF	11.7 (3.6)	9.2 (3.4)	10.4 (4.6)	10.3 (4.1)	11.3 (3.0)	7.9 (4.3)
DBW	10.7 (4.2)	8.1 (3.4)	9.5 (4.6)	9.8 (4.7)	10.5 (3.7)	7.3 (4.5)
HF& DBW	11.7 (4.1)	8.8 (2.9)	10.8 (4.4)	9.3 (4.5)	11.9 (4.3)	8.0 (4.2)

B. Subjective Evaluation

The NASA TLX was selected as the subjective questionnaire because it is extensively used and validated in diverse human-machine systems domains, although other evaluation methods exist (e.g., DALI [31]). Table II shows the results of the NASA TLX, revealing only small differences between setups. The DBW setup resulted in less temporal demand ($p=0.004$) and less effort than no support did ($p=0.003$), although this difference may be caused by a learning effect. Perceived performance did not significantly differ between setups, while objective performance indicated that the DBW setups reduced the number of road departures but increased the occurrence of hits with the pylons at $y = 1$ m for the DBW setups (see Table I, DBW and DBW & HF).

IV. DISCUSSION

We developed a road departure prevention (RDP) system and tested it in an emergency scenario. Thirty participants were instructed to avoid a pylon-confined area (representing an obstacle) while keeping the vehicle inside the road limits. The RDP system intervened when a road departure was likely to occur by applying a low level of automation in the form of advisory HF torque, and/or a high level of automation by correcting the front-wheels angle (DBW and DBW & HF).

HF had a profound influence on the measured steering torque, but no significant influence on steering-wheel angle or vehicle path. Apparently, in an emergency situation, drivers steer in an open-loop fashion without much regard for additional feedback torques that are applied on the steering wheel. That is, drivers used the best of their abilities to avoid an obstacle in an emergency, showing little inclination to give way to advisory steering-wheel torques. Note that the applied torques may have been too small to be able to override or guide the drivers' intentions and a higher feedback force may be needed to effectively prevent road departure in this evasive maneuver. However, higher magnitude HF torques in preliminary tests were perceived as authoritarian and were discarded to promote driving comfort and safety.

The DBW setups virtually eliminated road departures (see Fig. 5 and Table II) and tended to reduce self-reported workload. However, DBW, which influenced the relationship between steering-wheel angle and front-wheels steering angle, resulted in drivers hitting the inner pylons. This may be related to the fact that drivers did not perceive the operating principle of the RDP (which was explained to them prior to testing). Stimulus-response compatibility was degraded with the DBW systems, that is, steering response stopped being unambiguously related to steering-wheel angle, an approach

which may confuse the driver and disrupt his/her internal model of the vehicle.

This study is the first to address a high level of automation in the form of a DBW concept for RDP in emergency scenarios. We conclude that a DBW setup can prevent road departure, reduce self-reported workload, and has the potential to promote safety. If DBW RDP controllers are adopted in real vehicles, they should be designed to avoid or compensate for inadvertent driver reactions to RDP interventions. Careful design and rigorous testing should be the minimum precaution before DBW RDP controllers hit the road.

The technological challenges to bring RDP systems in production vehicles have already been addressed by the automotive community. The HF approach is similar to lane-keeping assist systems [4], [5] employing electrically power-assisted steering (EPAS) systems and cameras to detect the road markings. The benefits of EPAS systems in terms of fuel economy, weight-space saving, and reduced manufacturing-service cost, compared to traditional hydraulic power-assisted steering systems, have promoted EPAS even into pronounced sport vehicles [32]. The DBW approach would necessitate steering systems that decouple the driver's steering input and the front-wheels road angle. According to Nissan-Infiniti, such systems will be on sale in 2013 [33].

We feel that road safety will come through revolution in the automotive infrastructure rather than evolution on current safety systems [34]. The elimination of road crashes will only come through autonomous vehicles; accomplishing this technological milestone will likely invoke intermediate leaps, and DBW technology is envisioned to be one of them.

ACKNOWLEDGMENT

The authors would like to thank the test participants.

REFERENCES

- [1] J. S. Jermakian, "Crash avoidance potential of four passenger vehicle technologies," *Accid. Anal. Prevent.*, vol. 43, no. 3, pp. 32–40, Nov. 2010.
- [2] C. Schweinsberg. (2007). *Infiniti lane departure prevention to debut on new M, EX* [Online]. Available: http://wardsauto.com/ar/infiniti_lane_prevention
- [3] R. Rajamani, *Vehicle Dynamics and Control*. Berlin, Germany: Springer, 2006, pp. 17–18.
- [4] Japanvehicles.com. (2002, Sep.). *Toyota Caldina 2WD/4WD* [Online]. Available: <http://www.japanvehicles.com/newcars/toyota/Caldina/main.htm>
- [5] Honda World News. (2003, Jun.). *Honda announces a full model change for the inspire* [Online]. Available: http://world.honda.com/news/2003/4030618_2.html
- [6] K. A. Braitman, A. T. McCart, D. S. Zuby, and J. Singer, "Volvo and Infiniti drivers' experiences with select crash avoidance technologies," *Traffic Injury Prevent.*, vol. 11, no. 3, pp. 270–278, 2010.

- [7] EuroNCAP. (2013, Apr.). *Infiniti departure prevention system* [Online]. Available: http://www.euroncap.com/rewards/infiniti_ldp.aspx
- [8] D. LeBlanc, J. Sayer, C. Winkler, R. Ervin, S. Bogard, J. Devonshire, M. Mefford, M. Hagan, Z. Bareket, R. Goodsell, and T. Gordon, "Road departure crash warning system field operational test: Methodology and results," vol. 1, Univ. Michigan Transp. Res. Inst., Ann Arbor, MI, USA, Tech. Rep. UMTRI-2006-9-1, Jun. 2006 [Online]. Available: http://www.nhtsa.gov/DOT/NHTSA/NRD/Multimedia/PDFs/Crash%20Avoidance/2006/RDCW-Final-Report-Vol-1_JUNE.pdf
- [9] J. M. Chun, G. Park, S. Oh, J. Seo, S. H. Han, and S. Choi, "Evaluating the effectiveness of haptic feedback on a steering wheel for forward collision and blind spot warnings," in *Proc. 9th Pan-Pacific Conf. Ergonom.*, 2010 [Online]. Available: http://hvr.postech.ac.kr/wp-content/uploads/2010/03/IC52-JChun_PPCOE2010.pdf
- [10] S. de Groot, J. C. F. de Winter, J. M. L. García, M. Mulder, and P. A. Wieringa, "The effect of concurrent bandwidth feedback on learning the lane-keeping task in a driving simulator," *Human Factors*, vol. 53, no. 1, pp. 50–62, Feb. 2011.
- [11] P. G. Griffiths and R. B. Gillespie, "Sharing control between human and automation using haptic interface: Primary and secondary task performance benefits," *Human Factors*, vol. 47, no. 3, pp. 574–590, Fall 2005.
- [12] M. Mulder, D. A. Abbink, and E. R. Boer, "The effect of haptic guidance on curve negotiation behaviour of young, experienced drivers," in *Proc. IEEE Int. Conf. Syst., Man, Cybern.*, Oct. 2008, pp. 804–809.
- [13] M. Della Penna, M. M. van Paassen, D. A. Abbink, M. Mulder, and M. Mulder, "Reducing steering wheel stiffness is beneficial in supporting evasive maneuvers," in *Proc. IEEE Int. Conf. Syst., Man, Cybern.*, Oct. 2010, pp. 1628–1635.
- [14] J. C. F. de Winter and D. Dodou, "Preparing drivers for dangerous situations: A critical reflection on continuous shared control," in *Proc. IEEE Int. Conf. Syst., Man, Cybern.*, Oct. 2011, pp. 1050–1056.
- [15] D. A. Abbink and M. Mulder, *Advances in Haptics*. Rijeka, Croatia: InTech, Apr. 2010, pp. 499–516.
- [16] T. Inagaki, "Adaptive automation: Sharing and trading of control," in *Handbook of Cognitive Task Design*. Boca Raton, FL, USA: CRC, 2003, ch. 8, pp. 147–170.
- [17] T. Inagaki and T. B. Sheridan, "Authority and responsibility in human-machine systems: Probability theoretic validation of machine-initiated trading of authority," in *Cognition, Technology & Work*. Berlin, Germany: Springer, 2001, pp. 1–9.
- [18] C. Grover, I. Knight, F. Okoro, I. Simmons, G. Couper, P. Massie, and B. Smith, "Automated emergency brake systems: Technical requirements, costs and benefits, European Commission," TRL Ltd., Wokingham, U.K., Tech. Rep. PPR-227, Contract ENTR/05/17.01, Apr. 2008 [Online]. Available: http://ec.europa.eu/enterprise/sectors/automotive/files/projects/report_aebs_en.pdf
- [19] B. Seppelt, M. Lees, and J. Lee, "Driver distraction and reliance: Adaptive cruise control in the context of sensor reliability and algorithm limits," in *Proc. 3rd Int. Driving Symp. Human Factors Driver Assessment, Training Veh. Des.*, 2005, pp. 255–261.
- [20] N. Stanton and P. Marsden, "From fly-by-wire to drive-by-wire: Safety implications of automation in vehicles," *Safety Sci.*, vol. 24, no. 1, pp. 35–49, 2008.
- [21] M. Itoh, T. Horikome, and T. Inagaki, "Design and evaluation of situation-adaptive pedestrian-vehicle collision avoidance system," in *Proc. IEEE Int. Conf. Syst., Man, Cybern.*, Oct. 2011, pp. 1063–1068.
- [22] J. P. Switkes, E. J. Rossetter, I. A. Coe, and J. C. Gerdes, "Handwheel force feedback for lanekeeping assistance: Combined dynamics and stability," *J. Dynam. Syst. Meas. Control*, vol. 128, no. 3, pp. 532–542, 2006.
- [23] M. Alirezaei, M. Corno, D. Katzourakis, A. Ghaffari, and R. Kazemi, "A robust steering assistance system for road departure avoidance," *IEEE Trans. Veh. Technol.*, vol. 61, no. 5, pp. 1953–1960, Jun. 2012.
- [24] V. Cerone, M. Milanese, and D. Regruto, "Combined automatic lane-keeping and driver's steering through a 2-DOF control strategy," *IEEE Trans. Control Syst. Technol.*, vol. 17, no. 1, pp. 135–142, Jan. 2009.
- [25] D. I. Katzourakis, M. Alirezaei, J. C. F. de Winter, M. Corno, R. Happee, A. Ghaffari, and R. Kazemi, "Shared control for road departure prevention," in *Proc. IEEE Int. Conf. Syst., Man, Cybern.*, Oct. 2011, pp. 1037–1043.
- [26] D. I. Katzourakis, D. A. Abbink, R. Happee, and E. Holweg, "Steering force-feedback for human machine interface automotive experiments," *IEEE Trans. Instrum. Meas.*, vol. 60, no. 1, pp. 32–43, Jan. 2011.
- [27] S. G. Hart and L. E. Staveland, "Development of NASA-TLX (task load index): Results of empirical and theoretical research," in *Human Mental Workload*, P. A. Hancock and N. Meshkati, Eds. Amsterdam, The Netherlands: North Holland, 1988, pp. 139–183 [Online]. Available: <http://tos.pp.fi/koukku/892403.pdf>
- [28] J. C. F. de Winter, M. Mulder, M. M. van Paassen, D. A. Abbink, and P. A. Wieringa, "A two-dimensional weighting function for a driver assistance system," *IEEE Trans. Syst., Man, Cybern. B, Cybern.*, vol. 38, no. 1, pp. 189–195, Feb. 2008.
- [29] W. J. Conover and R. L. Iman, "Rank transformations as a bridge between parametric and nonparametric statistics," *Amer. Statist.*, vol. 35, no. 3, pp. 124–129, 1981.
- [30] J. D. Gibbons, *Nonparametric Statistical Inference*, 2nd ed., New York, NY, USA: Marcel Dekker, 1985, pp. 437–438.
- [31] A. Pausie, "Evaluating driver mental workload using the driving activity load index (DALI)," in *Proc. Eur. Conf. Human Interface Design Intell. Transp. Syst.*, 2008, pp. 67–77.
- [32] H. Rubinovich. (2011, Nov.). *Evo magazine U.K.—Driven: All-new Porsche 911 Carrera S* [Online]. Available: http://www.evo.co.uk/carreviews/evocarreviews/275107/driven_allnew_porsche_911_carrera_s.html
- [33] Nissan, *Nissan pioneers first-ever independent control steering technology: To be on sale within a year*, Oct.–Dec. 2012 [Online]. Available: http://www.nissan-global.com/EN/NEWS/2012/_STORY/121017-02-e.html
- [34] D. Katzourakis, "Driver steering support interfaces near the vehicle's handling limits," Ph.D. dissertation, Dept. Biomech. Eng., Faculty of Mechanical, Maritime and Materials Engineering, Delft Univ. Technol., Delft, The Netherlands, Jun. 20012 [Online]. Available: http://www.evo.co.uk/carreviews/evocarreviews/275107/driven_allnew_porsche_911_carrera_s.html
- [35] [Online]. Available: http://www.nissan-global.com/EN/NEWS/2012/_STORY/121017-02-e.html
- [36] [Online]. Available: <http://repository.tudelft.nl/view/ir/uuid:87f43ef4-c94a-43f1-8c24-d487b387ebbb/>



Diomidis I. Katzourakis received the Dipl. Ing. degree in computer engineering and informatics from the University of Patras, Patras, Greece in 2006, the M.Sc. degree in electronics from the Department of Electronic and Computer Engineering, Technical University of Crete, Chania, Greece, in 2008, and the Ph.D. degree on driver steering support interfaces near the vehicle's handling limits from the Department of BioMechanical Engineering, Faculty of Mechanical, Maritime and Materials Engineering, Delft University of Technology, Delft, The Netherlands, in

2012.

In 2011, he was a Research Contractor at Prodrive Automotive, U.K. He is currently a CAE Vehicle Dynamics Engineer at Volvo Cars Corporation, Göteborg, Sweden.



Joost C. F. de Winter received the M.Sc. degree in aerospace engineering and the Ph.D. degree in the field of driver training and assessment, both from the Delft University of Technology (TU Delft), Delft, The Netherlands, in 2004 and 2009, respectively.

He is currently an Assistant Professor at the Department of BioMechanical Engineering, Faculty of Mechanical, Maritime and Materials Engineering, TU Delft.



Mohsen Alirezaei received the M.Sc. degree in mechanical engineering from the Iran University of Science and Technology, Tehran, Iran, in 2006, and the Ph.D. degree in mechanical engineering/robotics and control from the K. N. Toosi University of Technology, Tehran, in 2011.

He is currently a Post-Doctoral Researcher at the Delft Center for System and Control, Faculty of Mechanical, Maritime and Materials Engineering, Delft University of Technology, Delft, The Netherlands.



Matteo Corno jointly received the M.Sc. (*cum laude*) degree in computer and electrical engineering from the University of Illinois at Chicago, Chicago, IL, USA, and the Laurea (*cum laude*) degree from the Politecnico di Milano, Milan, Italy, in 2005, and the Ph.D. (*cum laude*) degree on active stability control of two-wheeled vehicle from the Politecnico di Milano in 2009.

While pursuing the Ph.D. degree, he was a Guest Researcher at Alenia Spazio (now Thales Alenia Space), University of Minnesota and Harley-

Davidson. After a joint post-doctoral position at the Politecnico di Milano and Johannes Kepler University, Linz, Austria, he joined the Delft Center for System and Control, Delft University of Technology, Delft, The Netherlands, in 2009, as an Assistant Professor. His current research interests include dynamics and control of two- and four-wheeled vehicles, nonlinear estimation techniques, and linear parametric varying control.



Riender Happee received the M.Sc. degree in mechanical engineering and the Ph.D. degree from the Delft University of Technology (TU Delft), Delft, The Netherlands, in 1986 and 1992, respectively.

As a Product Manager and Research Manager, he introduced biomechanical human models for impact and comfort simulation for the automotive market. Since 2007, he has been an Assistant Professor at TU Delft, where he leads automotive projects on human-machine interfacing for extreme driving, cooperative driving, automated driving, driving-

simulator fidelity and driver observation, and biomedical projects on neuromuscular stabilization of the neck and the lumbar spine.